DOI: 10.1002/chem.200701736

# Templated Growth of Hybrid Structures at the Peptide–Peptide Interface

**Surajit Ghosh and Sandeep Verma*[a]**

**Abstract:** This study describes the use of peptide vesicular platforms for the templated growth of fibrillar structures to craft hybrids that retain the gross morphological features of two discreet self-assembled peptides. A synthetic triskelion peptide, which results in the rapid emergence of self-assembled spherical structures, was employed as a template. Addition of either one of two different peptides, both of which form long filamentous structures when co-incubated with the triskelion solution, affords hybrids that retain the gross morphology of both the spherical and filamentous structures. It is surmised that this process is aided by hydrogen bonding and the interdigitation of aromatic residues, which leads to the growth of hybrid structures. We believe that observations concerning the surface-assisted growth of peptide fibrils and tubular structures from vesicular platforms may have ramifications for the design and development of peptide-based hybrid materials with controlled hierarchical structures.

**Keywords:** fibers · fluorescence · peptides · pi interactions · vesicles

## Introduction

The controlled growth of hybrid superstructures follows the considerable progress made on the study of molecular self-assembly processes that are aided by various noncovalent interactions. The design and growth of such hybrid structures involves the complex interplay of both intermolecular and molecule–substrate interactions that, in turn, exert substantial influence and control over surface-templated growth. Such hybrid structures not only afford a variety of supramolecular ensembles, but may also be tuned to mimic the functions and properties of natural biomolecules.[1]

Peptides and proteins support the formation of supramolecular architectures by the participation of a variety of noncovalent intermolecular interactions, such as backbone hydrogen bonding, salt bridges, side-chain interactions, and stereochemical predispositions.[2,3] For example, the interactions that arise from the chemical diversity of amino acid side chains are crucial for amyloid organization through side chain–side chain and backbone–side chain interactions.[3c,e] Thus, it is possible to use noncovalent interactions to construct interesting architectures on pre-existing templates. Herein, we describe the use of peptide vesicular platforms for the templated growth of fibrillar structures to create hybrid structures that retain the overall gross morphological features of two discreet self-assembling systems.

## Results and Discussion

**Synthesis, sample preparation, and molecular structure**: Peptides **A**, **B**, and **C** (Figure 1) were prepared by using a routine solution-phase method. Recently, we presented the formation of homogeneous spherical vesicular structures from a synthetic triskelion peptide conjugate (**A**; Figure 1a), in which three Trp–Trp dipeptides are arranged around a tris(2-aminoethyl)amine (tren) scaffold.[4] This facile process, in which the occurrence of spherical aggregates was observed within the first 5 seconds of the incubation period, was ascribed to stacking of the tryptophan indole rings, which plays an intriguing role in the self-assembly process. In another study, we demonstrated the propensity of conjugate **B** (Figure 1b) to form linear fibers in a time-dependent fashion.[5] With these two model systems that have distinct self-assembly patterns to hand, this study was designed to explore whether rapidly forming vesicular structures would support the surface-assisted growth of peptide fibers.

[a] S. Ghosh, Dr. S. Verma
Department of Chemistry
Indian Institute of Technology Kanpur
Kanpur, UP, 208016 (India)
Fax: (+91) 512-259-7643
E-mail: sverma@iitk.ac.in

Supporting information for this article is available on the WWW under http://www.chemeurj.org/ or from the author.

   

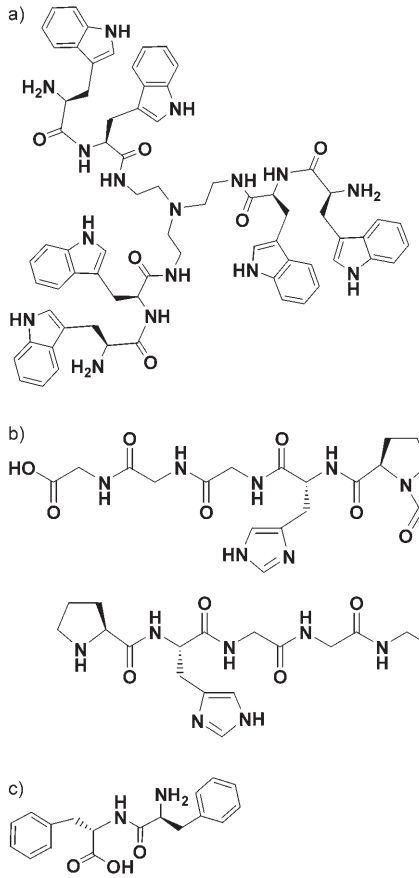


Figure 1. Molecular structures of a) triskelion peptide conjugate **A**, b) PHGGG-Cap-PHGGG **B** (Cap = 6-aminocaproic acid), and c) Phe–Phe dipeptide **C**.

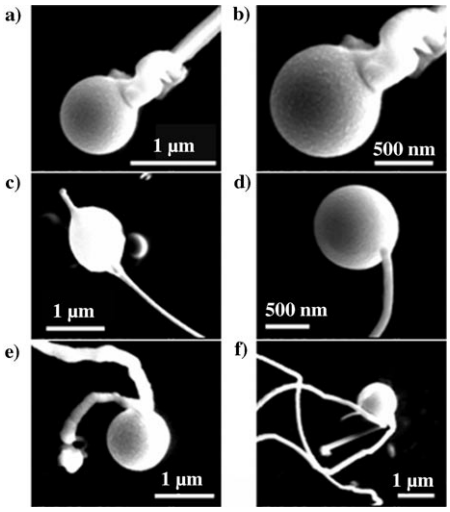


Figure 2. SEM images of the growth of fibers of **B** from the vesicle surface after different periods of incubation. a,b) After 3 d, c,d) after 7 d, and e,f) after 15 d.

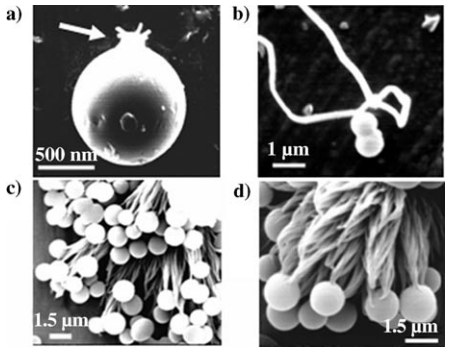


Figure 3. SEM images of the growth of fibers of **C** from the vesicle surface after different periods of incubation. a) After 3 d (arrowhead indicates nascent growth of fibers), b) after 10 d, and c,d) after 30 d.

**Ultrastructural details by microscopic studies**: A freshly prepared solution of **B** (0.33 mM) in 60% methanol/water was added to a solution of **A** (1 mM; 37 °C) that had been pre-incubated for 6 h, followed by incubation for up to 30 d. The phased growth of peptide fibers arising from the vesicular platform was followed by scanning electron microscopy (SEM). Observation of three-day-old solutions indicated that peptide fibers grow from the vesicular surfaces, and the length of these fibers increased with prolonged incubation (Figure 2a–d). After further incubation, growth and branching of new fibers from the surface was observed (Figure 2e and f). As spherical vesicles form rapidly upon dissolution, it was interesting to note that the preformed peptide surface provided a platform for fiber growth.

To provide further proof for this surface-assisted phenomenon, we decided to investigate the growth of tubular structures of Phe–Phe dipeptide **C** from a spherical platform. Dipeptide **C** (Figure 1c) forms robust tubular structures upon incubation and its use in other nanobiotechnological applications has been described.[6] Once again, growth of nanotubular structures from the vesicular surface was observed (Figure 3). We were able to capture snap-shots of the phased growth of hybrid structures after 3, 10, and 30 d. In the three-day-old solution (Figure 3a), the outgrowth of a nascent fiber from the surface was observed, which suggests that sequential growth, elongation, and consequently, dense fibrillation from the vesicular surface occurred (Figure 3b–d).

Environmental scanning electron microscopy (E-SEM) was used to follow the growth of these hybrid structures under moist conditions. Images obtained in this near-native state further confirmed the occurrence of fibrous growth from the vesicular platforms (Figure 4a), thereby suggesting that these observations reflect true surface-assisted growth rather than artifacts from drying. Transmission electron microscopy (TEM) images of seven-day-old samples revealed that two or more vesicles were interconnected by fibers and a micrograph of a 15-day-old sample displayed extensive fibril formation from the vesicular surfaces and dense interconnections between multiple vesicles (Figure 4b–d).

These observations were reconfirmed with results from atomic force microscopy (AFM) studies on seven-day-old samples. The initial phase of fibrous growth from the vesicle

  

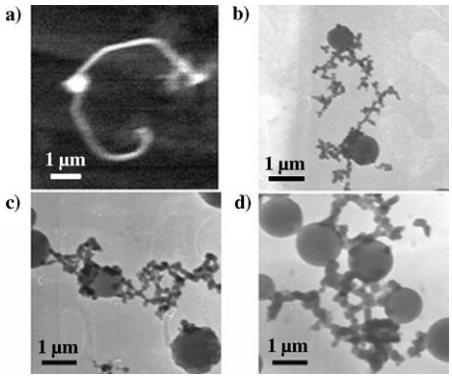


Figure 4. E-SEM and TEM images of the outgrowth of peptide **B** fibers from the vesicle surface after different periods of incubation. a) After 7 d (E-SEM), b) after 7 d (TEM), and c,d) after 15 d (TEM).

surface culminated in extensive fibrillation after 30 d (Figure 5a and b). Rhodamine B stained peptide solution (detected by fluorescence microscopy) also duplicated our observations (Figure 5c and d).

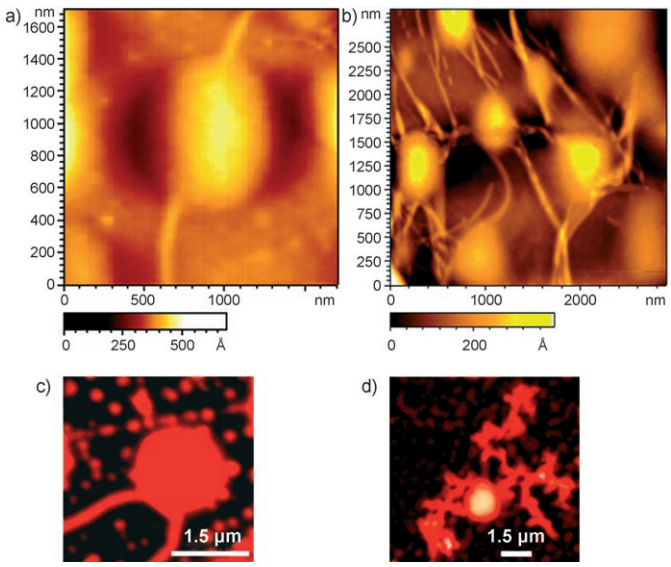


Figure 5. AFM micrographs after incubation for a) 7 and b) 30 d. Rhodamine B stained fluorescence micrographs after incubation for c) 7 and d) 15 d.

**Fluorescence studies**: Aromatic π–π stacking interactions between histidine and phenylalanine side chains and the indole ring of tryptophan have been reported,[7] and it is assumed that these interactions are primarily responsible for the templated growth of hybrid structures. In a preliminary experiment, we found that the intrinsic tryptophan fluorescence of **A** decreased upon the incremental addition of **B**, and also when the solution was incubated for seven days, which suggested a change in the tryptophan indole environment (Figures 6 and 7). In another control experiment, neither the addition of indole to **B** nor the addition of imidazole to **A** resulted in the formation of hybrid structures, thus implying the importance of peptide–peptide interactions (see the Supporting Information). Interfacial hydrophobicity and hydrophilicity have also been described as playing a role in certain self-assembling peptides and the structures they form.[8]

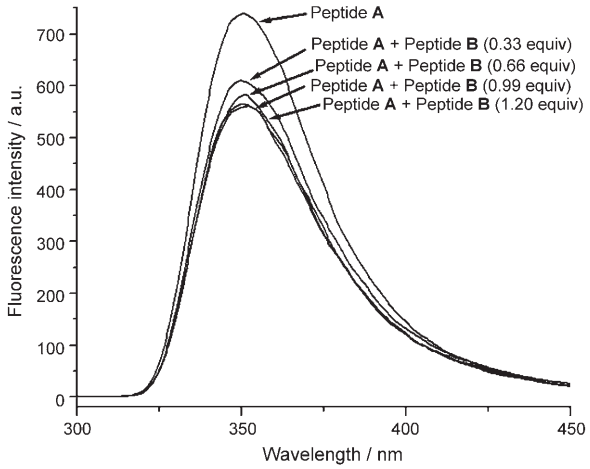


Figure 6. A comparison of fluorescence spectra shows the concentration-dependent quenching of the tryptophan fluorescence of **A** (1 μM) by the addition of **B** (0.33–0.99 equiv). Further addition of **B** (1.20 equiv) did not result in further quenching.

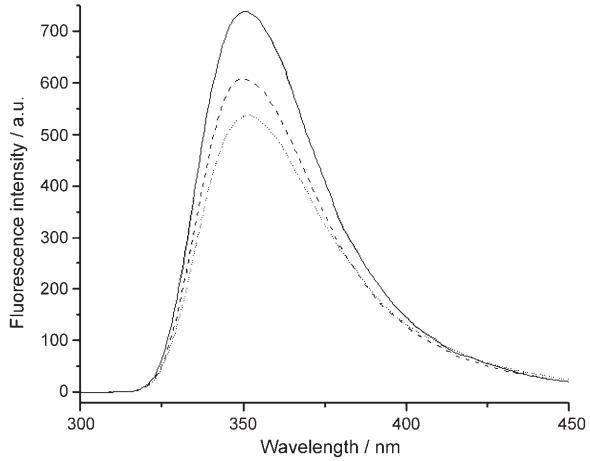


Figure 7. A comparison of fluorescence spectra shows the time-dependent quenching of the tryptophan fluorescence of **A** (1 μM) by the addition of **B** (0.3 equiv). ——: **A**. -----: **A+B**, no incubation. ·····: **A+B**, 7 d incubation.

Similar morphological observations have been made with an insulin–amyloid system, in which the growth of insulin fibers on preformed synthetic amyloid plaques was used to study the template-directed self-assembly process. It was found that template-driven fibril formation occurred at a highly accelerated rate, which resulted in thinner fibrils. This effect was attributed to limited nucleation sites on the template surface and lack of lateral twisting between fibrils.[9]

  

**Proposed schematic for hybrid structures**: It was proposed that the formation of vesicular structures in **A** is dictated by the tryptophan residues and tripodal tren scaffold.[4] MM+ calculations indicated that the tripodal scaffold imparts slight curvature and the π-stacked indole moieties of this conjugate interdigitate, which leads to the formation of stable vesicular structures. Therefore, we reason that the histidine imidazole and polymethylene linkers in **B** and the phenyl side chains in **C** may further interdigitate with the aromatic core of the vesicles to support the formation and growth of hybrid structures. Figure 8 depicts a possible mechanism for this process in which favorable interactions between the tryptophan indole groups (ovals) and the indole and phenyl groups (squares) of histidine and phenylalanine, respectively, are proposed.

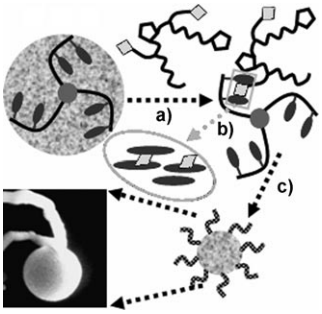


Figure 8. Proposed model that shows the growth of the hybrid structures: a) The interaction of vesicles with fiber-forming peptides, b) a detail of possible aromatic and hydrophobic interactions between side-chain residues and polymethylene linkers, and c) the growth of hybrid structures.

## Conclusion

This study describes the formation of peptide–peptide hybrids by combining the morphological signature of a synthetic triskelion derivative with two different peptide constructs. The ultrastructural features observed by microscopy analysis convincingly suggest that triskelion vesicles template the growth of hybrid structures, which have been well characterized by using fluorescence measurements and several microscopy techniques. It is also proposed that the formation of these hybrids is perhaps a result of the interplay of amide-hydrogen-bonding interactions within the hydrophobic environment created by the indole residues. We surmise that observations concerning the surface-assisted growth of peptide fibrils and tubular structures from vesicular templates may have ramifications for the design and development of peptide-based hybrid materials with controlled hierarchical structures. Such systems, with suitable noncovalent interactions, may also serve as materials for biosensor development and diagnostic applications.[10]

## Experimental Section

**SEM analysis**: Fresh and incubated (0–30 d) peptide solutions (20 μL, 0.33, 0.5, and 1 mM for **B**, **C** and **A**, respectively) in 60% methanol/water were coated onto metal slides and then a gold coating was applied over the samples. SEM measurements were performed by using an FEI QUANTA 200 microscope equipped with a tungsten filament gun. Micrographs were recorded at a working distance of 10.6 mm and at a magnification of 40000×.

**E-SEM analysis**: The mixed peptide solutions were placed on a metal stand and imaged by using an FEI QUANTA 200 microscope equipped with a field emission gun operating at 20.0 kV in wet mode at a pressure of 1.0 torr.

**TEM analysis**: An aliquot of incubated peptide solution (10 μL) was placed on a 400-mesh copper grid. After a minute, excess fluid was removed and the grid was stained with 2% uranyl acetate in water. Excess staining solution was removed from the grid after two minutes. Samples were viewed by using a JEOL 1200EX electron microscope operating at 80 kV.

**AFM analysis**: An aliquot of peptide solution (10 μL, incubation for 0–30 d) in 60% methanol/water was transferred onto a freshly cleaved mica surface and uniformly spread by using a spin-coater operating at 200–500 rpm (PRS-4000). The sample-coated mica was dried for 30 min at room temperature, then imaged by using an atomic force microscope (Molecular Imaging, USA) operating in acoustic AC mode (AAC) with the aid of a cantilever (NSC 12(c), MikroMasch). The force constant was 0.6 $N m^{-1}$ and the resonant frequency was 150 kHz. The images were recorded in air at room temperature, with a scan speed of 1.5–2.2 lines $s^{-1}$. Data were acquired by using PicoScan 5 software and data analysis was performed with the aid of a visual scanning probe microscopy program.

**Fluorescence microscopy**: Dye-stained peptide structures were examined by using a fluorescence microscope (Zeiss Axioskop 2 Plus) with an illuminator (Zeiss HBO 100) and a rhodamine filter (absorption 540 nm/emission 625 nm). This filter-optimized visualization compared rhodamine-treated vesicles (positive resolution) with untreated vesicles (negative resolution), which are virtually invisible in light of this wavelength. Images were captured electronically by using Zeiss AxioVision (version 3.1). Peptide **A** (1 mM) and rhodamine B (10 μM) were co-incubated for 24 h in 60% methanol/water before **B** (0.33 mM) was added, and the solution was then incubated for a further 7 d. This incubated solution (20 μL) was loaded onto a glass slide, dried at room temperature and the images were recorded.

**Fluorescence spectroscopy**: A freshly prepared solution of **A** (1 μM) in 60% methanol/water was used for the fluorescence measurements. Portions of peptide **B** (0.33–1.20 equiv) in 60% methanol/water were added and the intensity of the fluorescence was measured by using a Perkin–Elmer fluorimeter with an excitation wavelength of 275 nm, an excitation slit width of 8 nm, and an emission slit width of 10 nm. The pH of the solution was unchanged before and after the addition of **B**.

## Acknowledgements

We thank ACMS, IIT Kanpur, for access to microscopic facilities. S.G. thanks IIT-Kanpur for a pre-doctoral research fellowship and SV thanks DST, India, for financial support through a Swarnajayanti Fellowship.

[1] a) R. Baron, B. Willner, I. Willner, *Chem. Commun.* **2007**, 323–332; b) M. J. Kogan, I. Olmedo, L. Hosta, A. R. Guerrero, L. J. Cruz, F. Albericio, *Nanomedicine* **2007**, *2*, 287–306; c) L. C. Palmer, Y. S. Velichko, M. Olvera De La Cruz, S. I. Stupp, *Phil. Trans. Royal Soc.* **2007**, *365*, 1417–1433; d) D. Zanuy, R. Nussinov, C. Aleman, *Phys. Biol.* **2006**, *3*, S80–S90; e) M. A. B. Block, S. Hecht, *Angew. Chem.* **2005**, *117*, 7146–7149; *Angew. Chem. Int. Ed.* **2005**, *44*, 6986–6989; f) L.-Q. Wu, G. F. Payne, *Trends Biotechnol.* **2004**, *22*, 593–599.

[2] a) X. Zhao, S. Zhang, *Macromol. Biosci.* **2007**, *7*, 13–22; b) C.-J. Tsai, J. Zheng, D. Zanuy, N. Haspel, H. Wolfson, C. Aleman, R. Nussinov, *Proteins Struct. Funct. Bioinf.* **2007**, *68*, 1–12; c) C. H. Görbitz, *Chem. Eur. J.* **2007**, *13*, 1022–1031; d) D. W. Wendell, J. Patti, C. D. Montemagno, *Small* **2006**, *2*, 1324–1329; e) X. Zhao, S.

  

Zhang, *Chem. Soc. Rev.* **2006**, *35*, 1105–1110; f) K. Sanford, M. Kumar, *Curr. Opin. Biotechnol.* **2005**, *16*, 416–421; g) H.-A. Klok, *Angew. Chem.* **2002**, *114*, 1579–1583; *Angew. Chem. Int. Ed.* **2002**, *41*, 1509–1513.

[3] a) N. Y. Palermo, J. Csontos, M. C. Owen, R. F. Murphy, S. Lovas, *J. Comput. Chem.* **2007**, *28*, 1208–1214; b) V. Ramakrishnan, R. Ranbhor, A. Kumar, S. Durani, *J. Phys. Chem. B* **2006**, *110*, 9314–9323; c) A. Caflisch, *Curr. Opin. Chem. Biol.* **2006**, *10*, 437–444; d) K. V. Brinda, S. Vishveshwara, *Biophys. J.* **2005**, *89*, 4159–4170; e) D. Zanuy, K. Gunasekaran, B. Ma, H.-H. Tsai, C.-J. Tsai, R. Nussinov, *Amyloid* **2004**, *11*, 143–161.

[4] S. Ghosh, M. Reches, E. Gazit, S. Verma, *Angew. Chem.* **2007**, *119*, 2048–2050; *Angew. Chem. Int. Ed.* **2007**, *46*, 2002–2004.

[5] S. Ghosh, S. Verma, *J. Phys. Chem. B* **2007**, *111*, 3750–3757.

[6] a) N. Hendler, N. Sidelman, M. Reches, E. Gazit, Y. Rosenberg, S. Richter, *Adv. Mater.* **2007**, *19*, 1485–1488; b) M. Reches, E. Gazit, *Phys. Biol.* **2006**, *3*, S10–S19; c) M. Reches, E. Gazit, *Nat. Nanotechnol.* **2006**, *1*, 195–200; d) C. H. Görbitz, *Chem. Commun.* **2006**, *22*, 2332–2334; e) L. Adler-Abramovich, M. Reches, V. L. Sedman, S. Allen, Saul J. B. Tendler, E. Gazit, *Langmuir* **2006**, *22*, 1313–1320; f) Y. Song, S. R. Challa, C. J. Medforth, Y. Qiu, R. K. Watt, D. Pena, J. E. Miller, F. van Swol, J. A. Shelnutt, *Chem. Commun.* **2004**, *9*, 1044–1045; g) M. Reches, E. Gazit, *Science* **2003**, *300*, 625–627; h) C. H. Görbitz, *Chem. Eur. J.* **2001**, *7*, 5153–5159.

[7] a) F. L. Gervasio, P. Procacci, G. Cardini, A. Guarna, A. Giolitti, V. Schettino, *J. Phys. Chem. A* **2000**, *104*, 1108–1114; b) G. B. McGaughey, M. Gagne, A. K. Rappe, *J. Biol. Chem.* **1998**, *273*, 15458–15463; c) J. Fernandez-Ricio, A. Vazquez, C. Civera, P. Sevilla, J. Sancho, *J. Mol. Biol.* **1997**, *267*, 184–197; d) D. Bromme, P. R. Bonneau, E. Purisima, P. Lachance, S. Hajnik, D. Y. Thomas, A. C. Storer, *Biochemistry* **1996**, *35*, 3970–3979; e) C. A. Hunter, J. Singh, J. M. Thornton, *J. Mol. Biol.* **1991**, *218*, 837–846.

[8] a) F. Zhang, H.-N. Du, Z.-X. Zhang, L.-N. Ji, H.-T. Li, L. Tang, H.-B. Wang, C.-H. Fan, H.-J. Xu, Y. Zhang, J. Hu, H.-Y. Hu, J.-H. He, *Angew. Chem.* **2006**, *118*, 3693–3695; *Angew. Chem. Int. Ed.* **2006**, *45*, 3611–3613; b) C. Whitehouse, J. Fang, A. Aggeli, M. Bell, R. Brydson, C. W. G. Fishwick, J. R. Henderson, C. M. Knobler, R. W. Owens, N. H. Thomson, D. A. Smith, N. Boden, *Angew. Chem.* **2005**, *117*, 2001–2004; *Angew. Chem. Int. Ed.* **2005**, *44*, 1965–1968; c) T. Kowalewski, D. M. Holtzman, *Proc. Natl. Acad. Sci. USA* **1999**, *96*, 3688–3693.

[9] C. Ha, C. B. Park, *Biotechnol. Bioeng.* **2005**, *90*, 848–855.

[10] a) K. Enander, G. T. Dolphin, B. Liedberg, I. Lundstroem, L. Baltzer, *Chem. Eur. J.* **2004**, *10*, 2375–2385; b) Y. Geng, D. E. Discher, J. Justynska, H. Schlaad, *Angew. Chem.* **2006**, *118*, 7740–7743; *Angew. Chem. Int. Ed.* **2006**, *45*, 7578–7581.

Received: November 4, 2007
Published online: December 28, 2007

  